2012

Structural and magnetic characterization of colloidal CdMnS

REVISTA MEXICANA DE FISICA, COYOACAN, v. 58, n. 2, supl., Part 1-2, pp. 73-76, DEC, 2012
http://www.producao.usp.br/handle/BDPI/41610

Revista Mexicana de Física S **58** (2) 73–76 DICIEMBRE 2012

Structural and magnetic characterization of colloidal CdMnS

J.R.L. Fernandez[a], V.A. Chitta[b], X. Gratens[c], K. Krambrock[d], M. de Souza-Parise[e], V.N. Freire[f], P.C. Morais[g]
[a,e,g] *Universidade de Brasília, Instituto de Física, Brasília, Brazil.*
e-mail: jrlfernandez@yahoo.com
[b,c] *Universidade de São Paulo, Departamento Física de Materiais e Mecânica-FMT, São Paulo SP, Brazil.*
[d] *Universidade Federal de Minas Gerais, Departamento de Física, Belo Horizonte MG, Brazil.*
[f] *Universidade Federal do Ceará, Departamento de Física, Fortaleza CE, Brazil.*

Recibido el 25 de junio de 2010; aceptado el 6 de octubre de 2010

This paper reports on the synthesis (chemical co-precipitation reaction) and characterization (X-ray diffraction, magnetization, and electron paramagnetic resonance) of nanosized $Cd_{1-x}Mn_xS$ particles with manganese concentration up to x = 0.73. Though the literature reports that nanosized (bulk) CdS can incorporate as much as 30% (50%) of manganese ion within its crystal structure we found manganese segregation at the nanoparticle surface at doping levels as low as 14%. We found that both XRD and magnetization data support the presence of the Mn_3O_4 phase (observed spin-glass transition around 43 K) at the high manganese doping levels whereas the EPR data strongly suggest preferential incorporation of manganese at the nanoparticle's surface, even at low manganese doping levels. Analyses of the experimental data strongly suggest the preparation of well-defined core/shell ($Cd_{1-x}Mn_xS/Mn_3O_4$) structures at higher levels of manganese doping.

Keywords: Colloidal CdS; manganese; spin-glass transition; structural and magnetic characterization.

En este trabajo reportamos el crecimiento (co-precipitación química en medio acuoso) y caracterización (difracción de rayos-X, medidas de magnetización y EPR) de nanopartículas de $Cd_{1-x}Mn_xS$ crecidas hasta la concentración de x=0.73. Aunque en la literatura esta reportado que nanopartículas (volumétrico) de CdS solamente pueden incorporar 30 % (50 %) de iones de manganeso en su estructura cristalina, nosotros encontramos segregación de átomos de manganeso en la superficie de las nanopartículas para concentraciones en la orden de 14 %. Medidas de rayos-X y magnetización detectaron la presencia de la fase correspondiente a Mn_3O_4 para las muestras dopadas con alta concentración de manganeso (fue observado a transición spin-glass para temperaturas próximas de 43 K). Además medidas de EPR surgieren la incorporación preferencial del manganeso en la superficie de la nanopartícula. Análisis de los datos experimentales surgieren fuertemente que las muestras crecieran en la forma de núcleo/envoltura ($Cd_{1-x}Mn_xS/Mn_3O_4$) cuando fueron crecidas con alta concentración de manganeso.

Descriptores: CdS coloidal; manganeso; transición vidrio de espín; caracterización estructural y magnética.

PACS: 75.50.Pp; 75.50.Tt; 75.75-c

1. Introduction

Transition-metal ions doped nanosized materials can be used to produce new ceramics, glasses, catalysts and materials for the optoelectronic industry, among others. Therefore, investigation of the very properties of materials which are tailored at the nanoscale dimension falls within the research priorities of different industrial segments nowadays. In particular, there is a huge interest in accessing the role played by the doping transition-metal ion in the growth dynamics of the hosting template. Furthermore, the knowledge of the transition-metal ion content that can be hosted by the nanosized structure as a function of its size plus the core/shell distribution of them is extremely important from both basic and applied point of views [1,2]. This information allows one to control the growth condition in order to manipulate and/or avoid phase separation and rich phase formation [3,4]. In the present study we report on the production of Mn-doped CdS nanoparticles as a function of the doping (Mn) content. The aim is to investigate the solubility profile of manganese within the CdS crystal structure at the nanoscale limit. Also, we report on the phase separation for the Mn-doped CdS samples at the high end of manganese content (above 14 % concentration). In addition to the points mentioned above this material system is quite interesting due to the possibility of spontaneous magnetic oxide formation at the nanoparticle surface, which allows developing hybrid systems incorporating both magnetic and optical properties.

2. Sample preparation

Analytic grade cadmium nitrate, ammonium sulfide and $MnCl_2$ reagents were purchased from VETEC (São Paulo, Brazil) and used as received without further purification. For the synthesis of $Cd_{1-x}Mn_xS$ nanocrystal 1.0 mol/L aqueous solutions of $(NH_4)_2S$ and $Cd(NO_3)_2$ + $MnCl_2$ were prepared separately. Co-precipitation chemical reactions were carried out mixing equal volumes of the as-prepared aqueous solutions. $Cd_{1-x}Mn_xS$ nanocrystal was precipitate at room temperature and under mechanical stirring. After precipitation the samples were centrifuged, washed with deionized water, and dried in vacuum at 10^{-3} mbar.

3. Results and discussion

Figure 1 shows the X-ray diffraction (XRD) spectra of the $Cd_{1-x}Mn_xS$ samples as a function of manganese concentra-

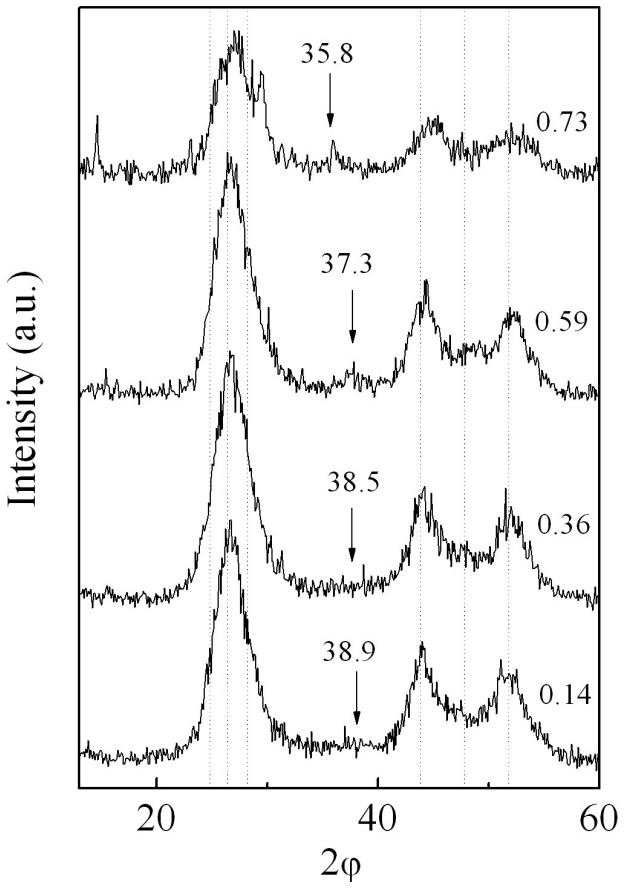

FIGURE 1. X-ray diffractograms recorded as a function of manganese concentration. Diffraction peaks around of 24.8°, 26.4°, 28.2°, 43.8°, 47.8° and 51.8° respectively correspond to the (100), (002), (101), (110), (103) and (112) reflections associated to the CdS Wurtzite phase. Arrows indicate the peak positions related to the Mn_3O_4 phase.

tion (x = 0.14-0.73). The XRD spectra confirm the typical CdS Wurtzite crystal structure [5,6] while the nanosized dimension is evidenced by the peak spectral broadening. Furthermore, all XRD spectra were monotonically shifted to the higher angle side as the Mn-content increases, thus indicating deformation of the CdS lattice parameter. This peak-shift is driven towards the lattice parameter of the MnS Wurtzite phase (γ-MnS) [7,8,9], though not following a linear dependence with the manganese content. Estimation of the particle diameter was accomplished by curve-fitting the XRD feature around of 26.7° using three Lorentzian-like components, assuming these components representing superposition of Wurtzite CdS peaks. The XRD peak fitting provides an average crystallite size around 4 nm. Finally, the XRD spectra show the onset of a new feature around 37° as the manganese concentration increases. The new XRD feature is well defined only at high manganese contents and its origin is claimed to be related to a new phase, namely Mn_3O_4.

To support to our assumption regarding the onset of the Mn_3O_4 phase Fig. 2 shows the XRD spectra of samples $Cd_{0.27}Mn_{0.73}S$ (a), γ-MnS (b),and oxidized γ-MnS (c).

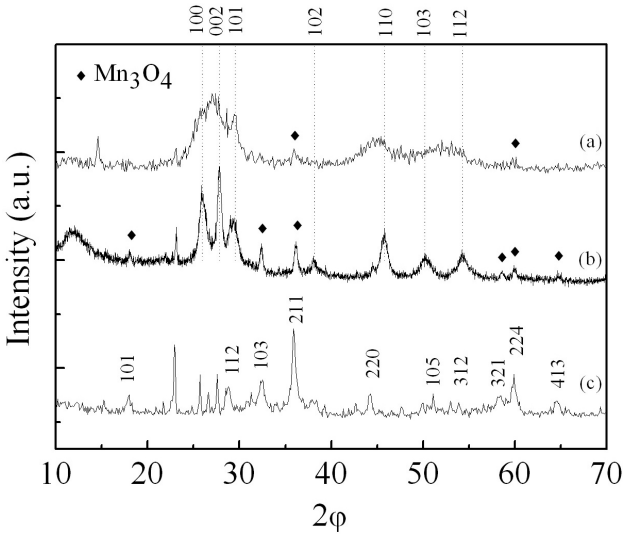

FIGURE 2. X-ray diffractograms of sample $Cd_{1-x}Mn_xS$ with x=0.73 (a), γ-MnS (b) and oxidized γ-MnS (c). Diffraction peaks around 25.9°, 27.8°, 29.5°, 38.2°, 45.8°, 50.2° and 54.2°, respectively correspond to the (100), (002), (101), (102), (110), (103) and (112) reflections due to the γ-MnS phase.

XRD data on Fig. 2(c) is basically Mn_3O_4 [10,11,12], which was obtained by the oxidation of γ-MnS. Notice that spontaneous oxidation of γ-MnS takes place as the sample is bring in contact with atmosphere air, at room temperature. Figure 2 clearly shows that the XRD spectrum in (a) is composed by CdS, γ-MnS, and Mn_3O_4. As discussed below additional magnetic measurements were performed in order to confirm the hypothesis of the Mn_3O_4 phase formation.

Figure 3 shows zero field cooled (ZFC) and field cooled (FC) magnetization measurements carried out on $Cd_{1-x}Mn_xS$ samples with x = 0.34 and x = 0.73. Both samples revealed a spin glass transition around 43 K, which agrees with the transition temperature of the Mn_3O_4 [13-16]. This magnetic transition is not well defined for the $Cd_{1-x}Mn_xS$ sample with x= 0.14 (data not shown). Indeed, both magnetic and XRD measurements support the onset of a new phase (Mn_3O_4) during the synthesis of nanosized $Cd_{1-x}Mn_xS$ particles. Furthermore, based on the XRD data we hypothesize that the Mn_3O_4 phase is formed at the nanoparticle surface and the Mn_3O_4 shell thickness depends upon the manganese concentration. We claim that this new phase (Mn_3O_4) responds for the distortion we observed on the CdS lattice parameter. From our experimental data we found evidences of phase separation in the $Cd_{1-x}Mn_xS$ material system at manganese concentration as low as 14%, which is much lower than the manganese solubility reported for CdS nanoparticles (around 30%) [1]. To access the information regarding the presence of Mn ions preferably at the nanoparticle surface, even at lower manganese doping, the $Cd_{1-x}Mn_xS$ sample with x = 0.00025 was investigated using electron paramagnetic resonance (EPR). Surface-uncapped and surface-capped (ethylene glycol coating) $Cd_{1-x}Mn_xS$ samples (x = 0.00025) were investigated. Room-temperature

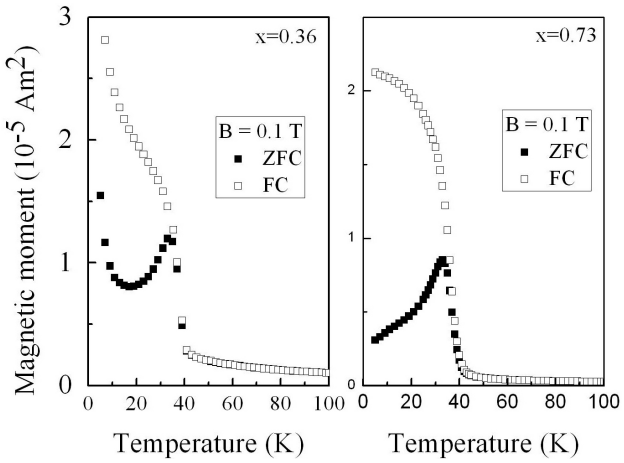

FIGURE 3. Zero field cooled and field cooled magnetic measurements of sample $Cd_{1-x}Mn_xS$ with x=0.36 and 0.73. Magnetic field of 0.1 Tesla was used for recording the data.

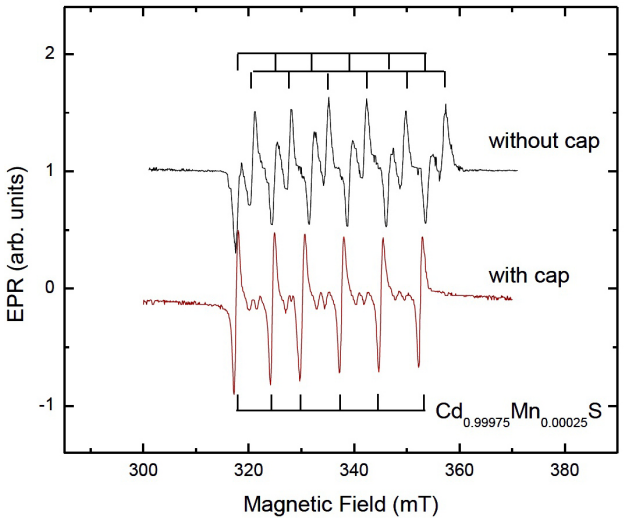

FIGURE 4. EPR spectra of capped (ethylene glycol) and uncapped $Cd_{1-x}Mn_xS$ samples for x = 0.00025.

EPR spectra of the investigated samples are shown in Fig. 4. The EPR spectra show different Mn-related spectra, depending of the sample preparation [4,17]. Three different local symmetries were found for the Mn^{2+} ions. The first EPR component is characterized by g = 2.001 and a = 204 MHz, which is associated to MnCd in the nanoparticle core. The second EPR component, with g = 2.001 and a = 290 MHz is due to Mn^{2+} near the nanoparticle surface (shell), which is suppressed by the ethylene glycol. The third EPR component provides g =1.981 and a = 204 MHz, being unstable and more likely related to the oxidation process taking place at the surface. These findings support the presence of Mn^{2+} ions, even at very light doping condition, preferably located at the nanoparticle surface and giving rise to the oxide-related phase.

4. Conclusions

Nanosized $Cd_{1-x}Mn_xS$ particles (x varying in a wide range) were successfully produced (co-precipitation chemical reaction) and characterized using XRD, magnetization measurements (ZFC and FC conditions), and EPR. Our findings indicate that particles are produced as well-defined core/shell structures at manganese concentration

below the limit of the reported value for manganese solubility (30%) in the hosting template (CdS). The shell layer, herein identified as Mn_3O_4, more likely growths during the material synthesis or immediately after the synthesis process due to the presence of oxygen in the reaction medium. The recorded EPR data strongly support the preference of the manganese ions for locating near the nanoparticle's surface.

Acknowledgements

J.R.L. Fernandez is supported by CNPQ process number 503533/2003-3.

1. S.C. Erwin, L. Zu,, M.I. Haftel, A.L. Efros, T.A., Kennedy, and D.J. Norris, *Nature* **436** (2005) 91.
2. D. Chen, R. Viswanatha, G.L. Ong, R. Xie, M. Balasubramaninan, and X. Peng, *J. Am. Chem. Soc.* **131** (2009) 93333.
3. S. Taguchi, A. Ishizumi, T. Tayagaki, and Y. Kanemitsu, *Applied Physics Letters* **94** (2009) 173101.
4. M.A. Malik, P. O'Brien, and N. Revaprasadu, *Journal of Materials Chemistry* **11** (2001) 2382.
5. Z.K. Heiba, *Powder Diffraction* **17** (2002) 191.
6. J.R.L. Fernandez, A. de Souza-Parise, and P.C. Morais, *Surface Science* **601** (2007) 3805.
7. Y.W. Jun, Y.Y. Jung, and J. Cheon, *J. Am. Chem. Soc.* **124** (2002) 615.
8. S.J. Lei,, K. Tang, Q. Yang, and H. Zheng, *European Journal of Inorganic Chemistry* **20** (2005) 4124.
9. Y. Zheng, Y. Cheng, Y. Wang, L. Zhou, F. Bao, and C. Jia, *J. Phys. Chem. B* **110** (2006) 8284.
10. A. Askarinejad, and A. Morsali, *Ultrasonics Sonochemistry* **16** (2009) 124.
11. H.Y. Xu, S. Xu, H. Wang, and H. Yan, *Journal of the Electrochemical Society* **152** (2005) C803.
12. L.X. Yang, Y.J. Zhu, H. Tong, W.W. Wang, and G.F. Cheng, *Journal of Solid State Chemistry* **179** (2006) 1225.
13. Na, C. W., Han, D. S., Kim, D. S., Park, J., Jeon, Y. T., Lee, G. and M.H. Jung, *Applied Physics Letters* **87** (2005) 142504.
14. J. Zhang, R. Skomski, and D.J. Sellmyer, *Journal of Applied Physics* **97** (2005) 10D303.

15. Z.H. Wang, D.Y. Geng, D. Li, and Z.D. Zhang, *J. Mater. Res.* **22** (2007) 2376.

16. R.K. Zheng, H. Liu, X.X. Zhang,, V.A.L. Roy, and A.B. Djurišiæ, *Applied Physics Letters* **85** (2004) 2589.

17. H. Zhou, D.M. Hofmann, H.R. Alves, and B.K. Meyer, *Journal Of Applied Physics* **99** (2006) 103502.